16èmes Journées de l'Hydrodynamique
27-29 novembre 2018 - Marseille

NAVIRE TRACTE PAR CERF-VOLANT : METHODOLOGIE POUR LES ESSAIS EN MER

BOAT TOWED BY KITE: METHODOLOGY FOR SEA TRIALS

M. BEHREL[(1)], K. RONCIN[(1)], P. IACHKINE[(2)], R. HASCOET[(1)], J.-B. LEROUX[(1)], F. MONTEL[(1)], Y. PARLIER[(3)]

kostia.roncin@gmail.com

[(1)]ENSTA Bretagne - IRDL UMR CNRS 6027, France
[(2)]ENVSN Quiberon, France
[(3)]Beyond the sea, ARCACHON, France

Résumé

Cet article présente des essais de propulsion par kite réalisé sur un bateau de 6 m spécialement dédié. Le pilotage du kite est automatique ou manuel, en mode dynamique ou statique selon l'allure. L'instrumentation permet de mesurer les mouvements du bateau et les efforts générés par le kite. Le dispositif de mesure du vent comprend des points ancrés dans la baie, et des mesures mobiles directement sur le kiteboat ou à proximité. Une modélisation fine au-dessus de la zone de mesure montre qu'une loi en puissance classique est insuffisante pour déterminer le vent au niveau du kite. Des phases systématiques de navigation d'une durée de 5 minutes ont été enregistrées. A l'issue de la campagne, 101 phases de navigation ont été réalisées. Les données sont traitées à l'aide d'une méthode de moyenne de phase. Les premiers résultats sont présentés.

Summary

This paper presents sea trials on a 6-meter boat specifically designed for kite propulsion. The kite control is automatic or manual, dynamic or static, depending on the point of sailing. The measurement system records boat motion and loads generated by the kite. A particular attention was payed for wind measurement with several fixed and mobile locations directly on the kiteboat or in the vicinity. A fine modelling shows that a classical power low is not satisfactory to describe the wind at kite location. 5-minute measurement phase were systematically recorded. At the end, 101 runs were conducted. Data are processed with the phase-averaging method in order to produce reliable results. First results are presented.

(a)

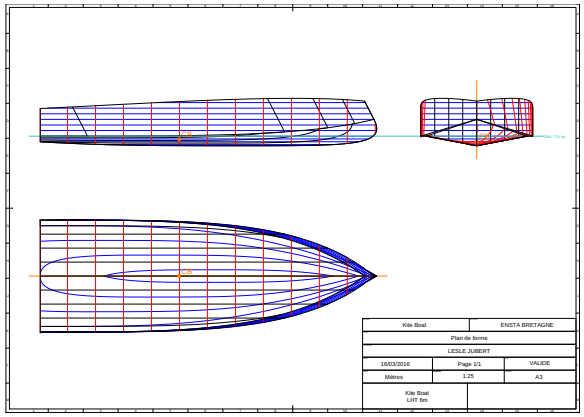

(b)

FIGURE 1 – (a) Kiteboat's wind measurement experimental set-up based on three sonic anemometers located at different altitude above sea level. (b) Planform of the KiteLab

I – Introduction

Research on kite have been essentially focused on electrical power production. Recently, kites have been investigated as an auxiliary propulsion for merchant ship [10, 3, 4, 7, 6]. Although there are few scientific publications on experiments carried out onshore, there is a lack of results for ships towed by kite. The aim of the present study is to provide a reliable database. A former attempt by [1] has shown the need for an instrumented ship, dedicated to this purpose. A 6-meter prototype has been designed and built (Fig. 1). An experimental device is deployed to ensure satisfactory assessment of the wind at kite position. The phase-averaging method developed by [2] is used in order to obtain precise and reliable results.

Kite Position. Within this study, only kite seen as a point is considered, with no motion of rigid body. This means that only the position of the kite is considered while its attitude is not measured. Therefore, three variables only are requested to position the kite. Because the kite is nearly flying on a sphere, spherical coordinates (r, θ, ϕ) are particularly suitable. However cartesian coordinates (Px, Py, Pz) are sometimes necessary.

II – Experimental set-up

II – 1 Kiteboat Specific Sensors

Most of the components were already integrated in the kite control box (see [2]) and in the two associated waterproof boxes, however a few sensors had to be fixed directly on the kiteboat. Onboard anemometers will be presented in SectionII – 2.

GPS and IMU. An IMU (Inertial Motion Unit) combined with a two GPS receivers provides boat orientations and velocities. This sensor is a VectorNav VN-300 Rugged. The two GPS receivers, in addition to provide position and velocities of the boat, give also an accurate heading measurement, apart from any magnetic interference.

Rudder Angle. A rudder angle based on a rotating potentiometer is included into the steering system. Calibrations were carried out at the laboratory, and zero balance is done

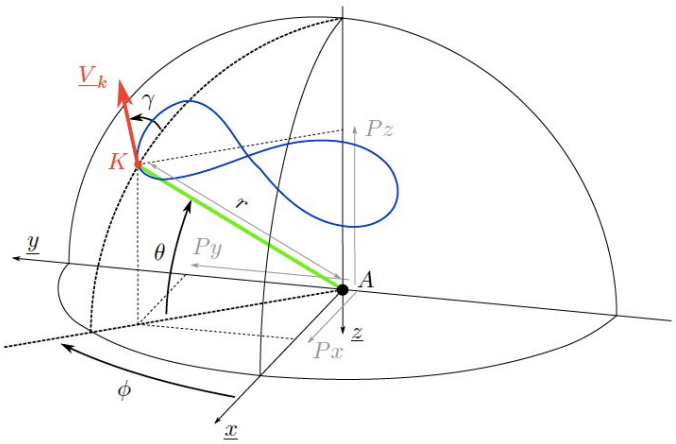

FIGURE 2 – Drawing of the two kite positioning systems : cartesian or spherical. The axis system used for positioning kite can vary depending on application.

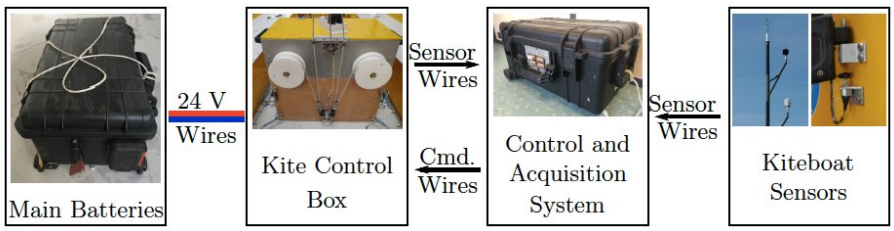

FIGURE 3 – Overview of the experimental set up when deployed on the kiteboat.

and checked several times a day.

II – 2 Wind Measurements.

Wind measurements are one of the most important aspects to compute post-processing. However, obtaining a good estimation of wind velocity at kite altitude is a complex task, particularly when measurements are done at sea.

Kiteboat Sytems. To get the wind over the kiteboat, three ultrasonic anemometers are fixed on the mast at three different altitudes. The three sonic anemometers are manufactured by Gill, but are from different models. The higher one, with a measurement altitude of 5.5 m above the sea level, is a WindMaster, a three dimensional sonic anemometer, fixed on the head of the mast, with a data flow rate of 20 Hz. The second one is a 2D anemometer WindSonic placed at 4.2 m above the sea level and deported from the mast by 0.6 m, with a data flow rate of 4 Hz. The last anemometer is a MaxiMet 500 (3.0 m above sea level, frequency 1Hz). A picture of the wind measurement mast mounted on the kiteboat is given in Fig. 1a.

Bay of Quiberon Systems. To ensure an even more accurate estimate of wind at kite position, a set of fixed measurement points was deployed in the bay of Quiberon, inspired from previous work [11, 7]. The system is based on 3 catamarans KL15, fitted with a five-meter mast with a 2D ultrasonic anemometer at the top. The sensor is a CV3F by LCJ Capteurs. A compass provides the heading of the platform. The GPS provides position

FIGURE 4 – Fixed wind measurement points deployed. Picture (a) shows the 4 measurement platforms. Picture (b) shows position of the 4 measurement points during trials (white circle) ; the central one is always occupied by the platform fitted with the 3-anemometer mast (on the right in picture (a)) ; the external locations are occupied by the others fitted with single-anemometer masts. The red circle shows the limit of the area of measurement (0.7 NM radius).

and absolute time, and it is used to synchronize data with the kiteboat acquisition system. Platforms location are given in Fig. 4 (b). A fourth catamaran KL15 is moored in the middle of the triangle formed by the three other catamarans. This one is fitted with the same wind measurement mast than the one mounted on the kiteboat and presented in the previous paragraph.

Sailing Area. The site which was chosen for the fieldwork is the bay of Quiberon (South Brittany, France). The sailing area of the bay of Quiberon is quite well documented in the literature [9, 7, 11]. The bay of Quiberon is surrounded by several wind sensors belonging to the Wind Morbihan network [1]. Experiments have been carried out in the area covered by the fixed-point wind sensors, shown in Fig. 4.

Overview of the Achievements. The fieldwork was carried out during a four-week period, 10 days with useful measurements (which was the initial target).This leads to 101 runs with a kite, in the sailing area. Adding to these ones the other specific runs like seakeeping or maneuverability tests, it finally corresponds to more than 9 hours and 40 minutes of relevant recordings. This required more than 80 hours on the water taking into account all steps of the trials. A video of presentation is available on YouTube [2].

III – Design of Experiments

A set of parameters were varied during the fieldwork from one run to another. The inputs of the matrix are described in the following paragraphs.

Kite. Three different kites are used : the two Cabrinha® kite with area of 5 and 12 m^2, and a third one built especially for the kiteboat by the beyond-the-sea company. This kite has an area of 5 m^2 , but it has been delivered only on the last two days of the sea trials.

1. http://windmorbihan.com/
2. https://www.youtube.com/watch?v=Zgd8KkaCavg

Symb.	Details
(COG)	Course Over Ground
V_s	Speed of the boat
ψ	Heading of the boat (HDG)
θ_s	Pitch angle of the boat
ϕ_s	Roll angle of the boat
δ_r	Rudder angle

(a)

Symb.	Details
$\underline{F}_m$	Front tether force vector
F_{bl}	Left back tether force
F_{br}	Right back tether force
$\lambda 1$	Position of actuator 1 (left)
$\lambda 2$	Position of actuator 2 (right)

(b)

TABLE 1 – Major variables recorded during runs. Table (a) presents information related to the boat, whereas part (b) deals with kite data.

True Wind Angle. Numerous true wind angles are tested, from upwind sailing with true wind angles about 60° , to full downwind (180°). The objective is to cover the range of true wind angle with an increment of 20°.

True Wind Speed. The magnitude of the wind is obviously a parameter that cannot be decided. Consequently, runs are done whatever the wind magnitude is, and they are then sorted to group together runs with similar wind magnitude.

Tether Lengths. Two set of tethers are considered, with lengths of 50 m and 80 m.

Kite Flight. For low true wind angles (lower than 80°), only static flight could be achieved. For medium true wind angles (between 80° and 100°), the dynamic flight was possible, but not with the automatic pilot. Indeed the kite needs to fly close to the wind window and the current autopilot is not able to deal efficiently with this type of situation. For larger true wind angle, from 100° to 180° , the autopilot presented in [2] based on the work by [5] controls the kite.

Kite Attachment Point. Four longitudinal positions of the kite attachment in the boat reference frame equally distributed along the boat were at first defined. However it became rapidly obvious that the extreme positions initially foresaw were in fact inoperable due to maneuverability issues. Finally one position was used most of the time, with a kite attachment point located at 2.68 m forward the transom.

Propulsion. Some of the runs are done with the outboard engine working. This allows upwind runs not always achievable with the kite alone. It also allows to consider the effect of kites on a motor boat, which is the purpose of the project.

IV – Available Data

Kiteboat Data. For each of the 101 runs recorded with kite , many data were recorded, and an overview of the most relevant ones is given in Tab.1.

Wind Data. A partnership has been engaged with the company EXWEXs specialized in weather forecast and weather models. The objective is to get a fine modeling (horizontal mesh size about 100 m, vertical mesh size of 20 m) of the wind over the sailing area, at high frequency (1.4 Hz), from 0 to 300m. Details on the models are given in a report with

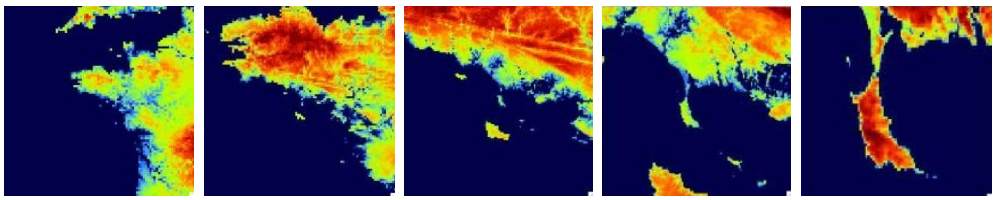

(a) Domain 1 (b) Domain 2 (c) Domain 3 (d) Domain 4 (e) Domain 5

FIGURE 5 – Spatial domains of the model used to predict the wind above the sailing area (Source : EXWEXs' report of modeling, [8]) .

the associated physic and outputs ([8]). The model in use is the Weather Research and Forecasting model (WRF, see [12]). The strategy of modeling for such a forecast is to nest several spatial domains centered on the area of interest, from the large one with largest horizontal resolution to the smallest one with the expected resolution of 110 m. The time step of the finest domain is equal to 0.72 s. The five domains, with their topography are presented in Fig. 5. Because a real time forecast is not necessary, initial conditions and boundary conditions were taken from reanalyzed data, coming from the National Center for Atmospheric Research (USA).

The outputs of the model are weather data along the altitude (from 20 m to 300 m) for 222 points of the grid spread over the sailing area and for each time step. The most interesting data, in our case, are the three components of the wind velocity, the temperature and the pressure. The results of a few hours of modeling outputted at the location of the center measurement platform are given in Fig. 6.

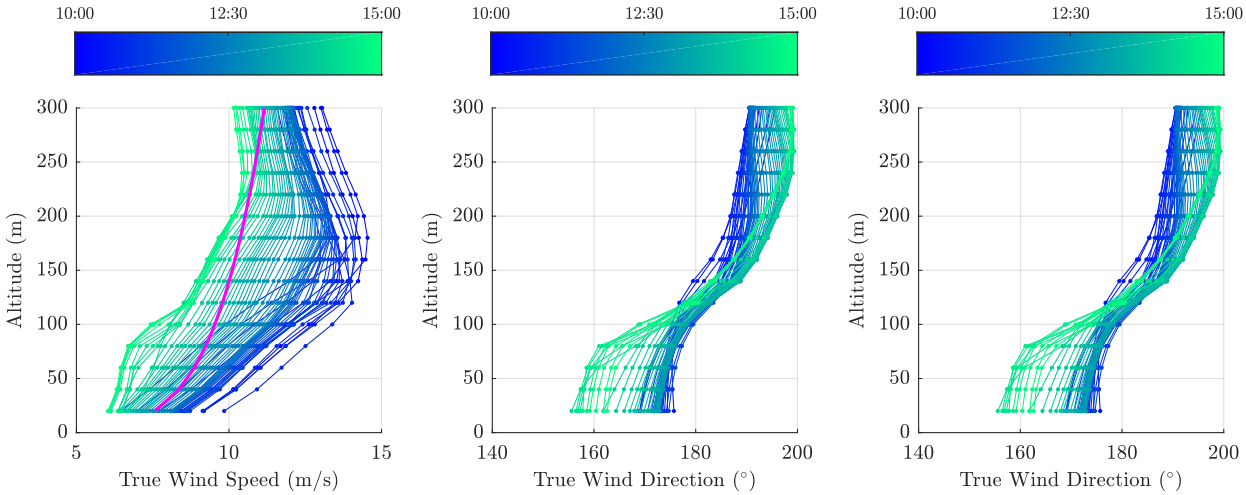

FIGURE 6 – Example of wind speed profile (a), wind direction profile (b) and vertical wind speed profile (c) calculated by the weather model during the 29th of March, and outputted at the location of the center measurement platform (time (UTC) of each profile depends on color, and is denoted by the colorbar). The magenta line on plot (a) denotes the ITTC profile, calculated from the average wind of all profile at 20 m during the period.

V – Wind Estimation at Kite Altitude

The post-processing of the kiteboat data is very close from the one presented in [2]. The present Section focuses on the different methods used to estimate the wind at kite altitude.

Power Law. The wind profile is fitted by a power-law of exponent 1/7. The limits of such a method have already been pointed out (see [2]). The difference between the weather modeling and the power law is shown in Fig. 6 (a).

Profiler Data. The SODAR used during the onshore work presented in [2] was also used during this work, but with a different purpose. Indeed, the SODAR was installed onshore in the ENVSN's facilities, and was there to get data in order to feed the weather model (introduced in Section IV). Therefore the settings were quite different from the ones used previously, leading to an altitude range of measurement going from 30 m to 600 m. The distance between the SODAR and the center of the sailing area was 2.5 NM.

Solution Based on the Profiles from the Weather Model. The first solution which is considered is to use the weather model to get a wind magnitude profile above the kiteboat, and then to scale this profile with measurements carried out on the kiteboat. In this case, no twist of the true wind direction along the altitude is assumed. The true wind direction is calculated with the data coming from the onboard sensors (anemometer for wind and GPS-IMU for boat velocity). However, the altitude of the onboard measurement of the wind and the altitude of the lowest point outputted by the model are not identical. Therefore, a wind estimate at the measurement point is linearly interpolated in time and space from the model data. A scale factor can be calculated, by dividing the measured value by the extrapolated one :

$$V_{WT}(z) = V_{WT,mod}(z) \overbrace{\frac{V_{WT,kb}(z_0)}{V_{WT,mod,extrap}(z_0)}}^{Scale\,Factor} \tag{1}$$

Solution Based only on the Data from the Weather Model. This last option is to directly interpolate the wind profile in the data provided by the model, without considering the measurements.

VI – First results

This section aims to point out some relevant elements regarding the global objective of the project. A representative case among the various trajectories achieved by the kite during the the 101 runs, is given in Fig. 7. The plot shows the trajectory of the kite flying in dynamic mode, and steered by the autopilot. This case is possible only for downwind and reaching conditions (true wind angles not smaller than 100° , see SectionIII), keeping in mind that autoplilot gives much better reproducibility than manual steering.

VI – 1 Benchmark of Redundant Wind Data

With the large number of sensors deployed for this work and presented in SectionII , some data are redundant. This enables to compare the sensors with each other, to check

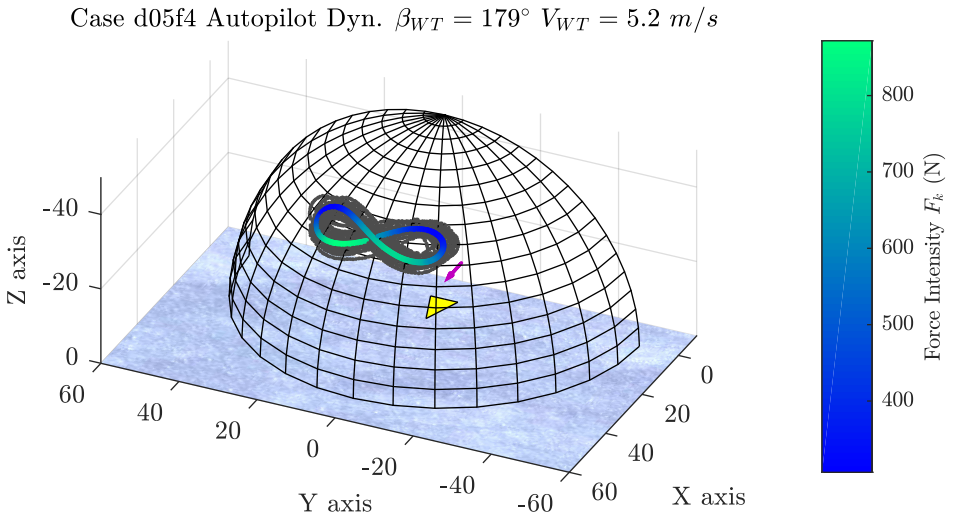

FIGURE 7 – Kite trajectory during a downwind run in black. The yellow triangle denotes the kiteboat position, and the magenta arrows give the orientation of the true wind. The trajectory processed by the phase-averaging method is colored in order to show the kite force with respect to its position.

their accuracy and possibly identify defective sensors. In the present paragraph we focus on onboard anemometers. Three anemometers are mounted on a dedicated mast, detailed in Section II – 2, at three different heights. Data coming from these three devices have also been compared, and an example of this work is given in Fig. 8 (a) . The correlation of the direction data (left plot) is very good. The plot of the true wind speed (right plot) shows that the uppers sensors measure stronger winds. This is consistent with boundary layer theory. Indeed, the average values of run for each sensors have been plotted with respect to the altitude of measurement and compared with the power law profile calculated from the highest measurement. Results are presented in part (b) of the same figure. In regard to these satisfactory agreements, the wind measured by the highest sensor (WindMaster) will be used when only one point of measurement is sufficient. This sensor being located at the top of the mast, there is no risk of blanketing effect. Moreover this sensor has a better output rate, and provides in addition a measurement along the vertical direction.

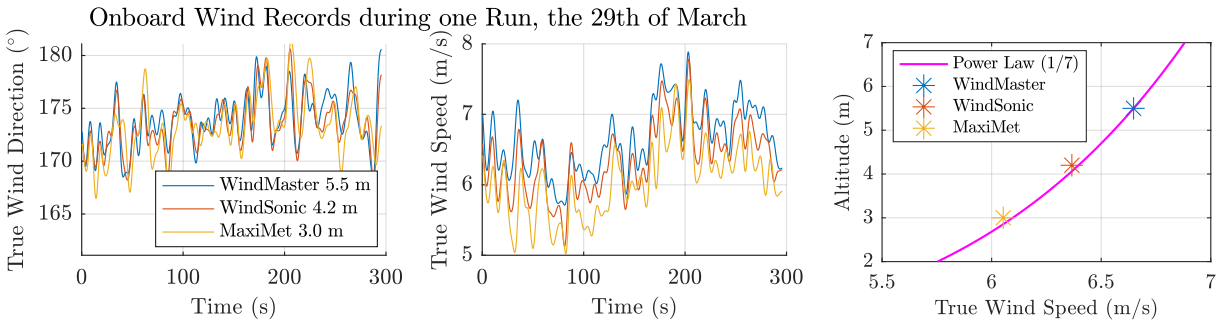

FIGURE 8 – Comparison between the wind measurements of the three onboard sensors (a). The average value of the true wind speed during the run is plotted for each one (b), and compared to the power law calculated from the WindMaster measurement at 5.5 m.

VI – 2 Average Data

For each of the 101 runs, data have been averaged. This allows to globally analyze the effects of parameters on the kiteboat performances and its behavior.

Back Tether Ratio. The ratio between the force in back tethers and the total kite force has been computed, as it has been done in [2], using the following formula :

$$r_b = \frac{F_{bl} + F_{br}}{F_{k,A}} \tag{2}$$

As expected, the ratio for the two Cabrinha kites are close to the ones obtained on-shore ([2]), with an average value of 23%. However this ratio for the third kite is quite different, with an average value of 40 %. This difference can be explained by regarding the special design of the BTS kite with an added line linking back and front bridle system.

Power Ratio. During the last two days of measurements, the main battery voltage has been recorded as well as the intensity of each channel of the power card. Therefore the electrical power P_e consumed by actuators can be analyzed. However the data rate was low (1 Hz), consequently a fine analysis of the consumption along a trajectory cannot be performed and only average values will be considered. This quantity is interesting to analyze, particularly in comparison with the propulsive power generated by the kite P_{prop}, which is the product of the propulsive force of the kite by the speed of the boat :

$$P_{prop} = V_s \underline{F}_{k,A} \cdot \underline{x}_\psi \tag{3}$$

The ratio of these two values, the 'power ratio', is denoted r_p :

$$r_p = \frac{P_{prop}}{P_e} \tag{4}$$

When this ratio is lower than 1, the control of the kite requires a level of power higher than the towing power provided. Results are given in Tab. 2. During these two days, runs have mostly been carried out in light wind with the BTS kite, with only 4 runs with the Cabrinha 12 m^2 . For runs with low true wind angles, the power ratio is close to 1 and even below for some runs. This is not surprising, because for these points of sail, most of the kite force is along the transverse axis of the boat, and consequently the propulsive force is low, so the power ratio. For greater true wind angles, the ratios increase, but remain relatively low for the BTS kite. On the contrary, the power ratios of the Cabrinha 12m^2 seem to be much better, but more data would be necessary with the Cabrinha kite to do a fair comparison. Further works have to be carried out to measure more accurately the power ratio. Note that the present steering system has not been designed with an energy efficiency approach.

VI – 3 Results processed with Phase-Averaging Method

The phase-averaging method, presented in [2], has been adapted to take into account the additional data induced by the boat. All the 101 runs are not suitable for the phase-averaging method. Indeed, a minimum reproducibility of the trajectories is required, and some sailing configurations do not allow such trajectories, as the manual steering. Finally 10 runs have been selected and results are presented in Tab.2. The back tether ratio r_b (Eq. 2) and the amplitude ratio r_a were already considered in [2]. The amplitude ratio

Case	Kite	β_{WT}	r_{prop}	r_a	r_b	r_s	$\triangle\delta_R$	$\triangle\psi$	$\triangle\phi_s$	$\triangle\theta_s$	$\triangle\delta$
d01f7	Cab. 5	137	0,76	1,28	0,20	0,13	12,1	2,4	4,7	1,3	0,75
d02f5	Cab. 12	182	0,47	0,90	0,19	0,11	8,2	3,1	1,5	0,8	0,87
d02f6	Cab. 12	182	0,67	0,96	0,20	0,10	2,9	4,2	2,0	1,0	0,85
d04f1	Cab. 12	183	0,62	0,95	0,22	0,09	4,1	3,9	1,6	0,6	0,66
d05f4	Cab. 12	179	0,69	1,12	0,20	0,11	4,2	2,8	1,9	0,5	0,92
d07f12	Cab. 12	121	0,60	2,00	0,21	0,34	7,8	4,7	3,8	1,4	0,91
d07f18	Cab. 12	263	0,31	1,80	0,23	0,31	12,0	18,6	10,7	0,8	0,97
d08f1	Cab. 12	180	0,80	1,34	0,22	0,16	4,7	1,4	1,5	0,7	1,07
d10f8	BTS	220	0,72	1,18	0,38	0,15	7,2	4,0	3,3	1,1	0,70
d11f4	BTS	106	0,49	1,22	0,40	0,14	12,9	6,2	4,0	1,9	0,73

TABLE 2 – Relevant quantities taken out from the ten runs suitable with the phase-averaging method. Angles are given in degree, and the steering amplitude is given in meter. The blue line denote the case which is plotted in Fig. 7 and 9.

is the amplitude of the force divided by the averaged force value along the trajectory. In addition, two others ratio are introduced here : the propulsive ratio r_{prop} and the amplitude speed ratio r_s. The first one denotes the part of the kite load useful for propulsion, i.e. the projection of the kite force on the x_ψ-axis :

$$r_{prop} = \frac{\underline{F}_{k,A} \cdot \underline{x}_\psi}{F_{k,A}} \tag{5}$$

The amplitude speed ratio denotes the maximum speed variation during the kite eight pattern in comparison with the average speed :

$$r_s = \frac{\max(V_s) - \min(V_s)}{\mu_{V_s}} = \frac{\triangle V_s}{\mu_{V_s}} \tag{6}$$

Moreover, other quantities are introduced denoting the variation of some parameters, as the amplitudes of the rudder angle $\triangle\delta_R$, of the heading angle $\triangle\psi$, of the roll angle $\triangle\phi_s$, of the pitch angle $\triangle\theta_s$ and the amplitude of the kite steering command $\triangle\delta$. The first three columns in Tab. 2 denote the short name of the case, the kite used and the true wind angle β_{WT}.

As an example one case was selected (Case d05f4 in Tab. 2). Results for this case are shown in Fig. 7 and 9. The variations of the lift to drag ratio and the lift coefficient along the trajectories are still not easy to interpret, with no generic scheme. The speed of the boat correlates with the propulsive force with a slight phase shift (inertia). The variations of the roll angle are clearly in line with the side force intensity. The stronger the side force is, the larger the amplitude of the roll angle. Such large side forces occur in reaching sailing conditions leading to roll angle over 10° (case d07f18).

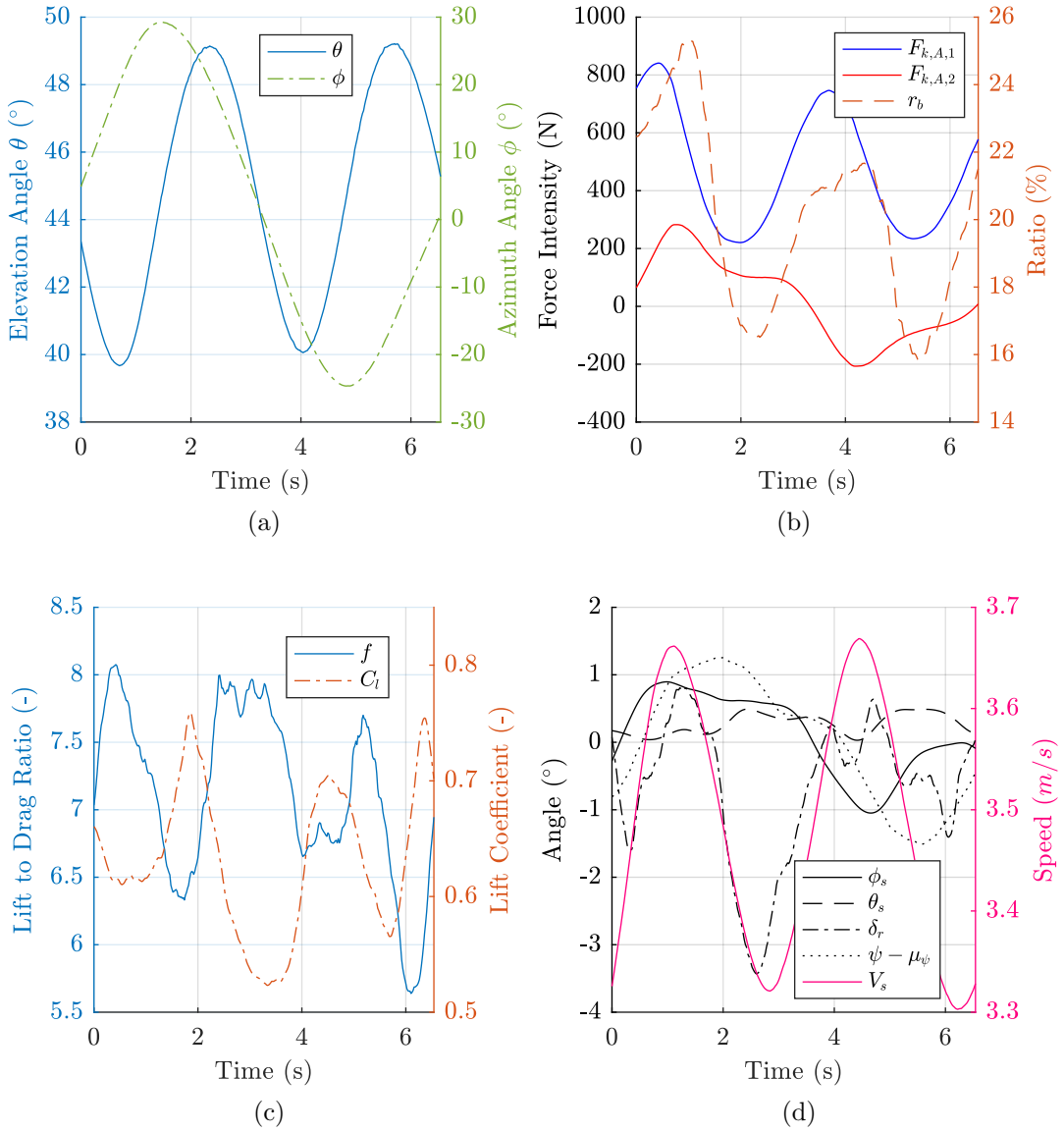

FIGURE 9 – Results of the phase-averaging process applied to a downwind run (case d05f4). (a) elevation and azimuth of the kite. (b) tension on back tethers and back tether ratio. (c) lift coefficient and lift to drag ratio of the kite. (d) attitude and speed of the boat.

VII – Conclusion

The objective of this experimental study was to acquire relevant data to analyse the behavior of a boat towed by a kite. These results could be used as a benchmark for models of kite-ship interations. The entire set of data has not been fully processed yet. Variations of kite characteristics along its eight trajectory are still not easy to interpret ; no generic trend could be outlined. By integrating wind data measurements carried out over the sailing area, into the weather model, the estimation of the true wind speed at kite altitude could be improved.

Acknowledgements

The authors are grateful to the French Environment & Energy Management Agency (ADEME) for funding this study.

Références

[1] M. Behrel, N. Bigi, K. Roncin, D. Grelon, F. Montel, A. Nême, J.-B. Leroux, C. Jochum, and Y. Parlier. Measured Performance of a 50-m2 Kite on a Trawler. In *10th Symposium on High-Performance Marine Vehicles (Hiper)*, pages 443–457, Cortona, ITALY, 2016.

[2] M. Behrel, K. Roncin, J.-B. Leroux, F. Montel, R. Hascoet, A. Neme, and C. Jochum. Application of phase averaging method for measuring kite performance : onshore results. *Journal of Sailing Technology*, (05) :1–29, 2018.

[3] G. M. Dadd. *Kite dynamics for ship propulsion.* PhD thesis, University of Southampton, 2013.

[4] M. Erhard and H. Strauch. Control of towing kites for seagoing vessels. *IEEE Transactions on Control Systems Technology*, 21(5) :1629–1640, 2013.

[5] L. Fagiano, A. U. Zgraggen, M. Morari, and M. Khammash. Automatic crosswind flight of tethered wings for airborne wind energy : modeling, control design and experimental results. *IEEE Transactions on Control Systems Technology*, 22(4) :1433–1447, 2014.

[6] R. Leloup, K. Roncin, M. Behrel, G. Bles, J.-B. Leroux, C. Jochum, and Y. Parlier. A continuous and analytical modelling for kites as auxiliary propulsion devoted to merchant ships, including fuel saving estimation. *Renewable Energy*, 86 :483–496, 2016.

[7] R. Leloup, K. Roncin, G. Bles, J.-B. Leroux, C. Jochum, and Y. Parlier. Kite and classical rig sailing performance comparison on a one design keel boat. *Ocean Engineering*, 90 :39–48, 2014.

[8] C. Messager. Rapport -2017-ENSTA-01. Technical report, EXWEXs, 2017.

[9] P. G. Mestayer, I. Calmet, O. Herlédant, S. Barré, T. Piquet, and J. Rosant. A coastal bay summer breeze study, part 1 : Results of the quiberon 2006 experimental campaign. *Boundary-Layer Meteorology*, 167(1) :1–26, Apr 2018.

[10] P. Naaijen, V. Koster, and R. P. Dallinga. On the power savings by an auxiliary kite propulsion system. *International Shipbuilding Progress*, 53(4) :255–279, 2006.

[11] K. Roncin, J.-M. Kobus, P. Iackine, and S. Barré. Méthodologie pour la validation du simulateur de voilier par des essais en mer , une première tentative. In *Workshop Science-Voile*, pages 1–10, Lanveoc-Poulmic, 2005.

[12] W. Skamarock, J. Klemp, J. Dudhi, D. Gill, D. Barker, M. Duda, X.-Y. Huang, W. Wang, and J. Powers. A Description of the Advanced Research WRF Version 3. Technical report, National Center for Atmospheric Research, Boulder, Colorado, USA, 2008.